ELSEVIER

Chemical Engineering Journal 139 (2008) 540–548

Chemical Engineering Journal

www.elsevier.com/locate/cej

Effect of enzyme molecules covering of oil–water interfacial area on the kinetic of oil hydrolysis

Sulaiman Al-Zuhair [a,*], K.B. Ramachandran [b], Masitah Hasan [c]

[a] *Department of Chemical and Petroleum Engineering, Faculty of Engineering, U.A.E. University, 17555 Al-Ain, United Arab Emirates*

[b] *Department of Biotechnology, Indian Institute of Technology Madras, Chennai 600036, India*

[c] *Department of Chemical Engineering, University of Malaya, 50603 Kuala Lumpur, Malaysia*

Received 1 June 2007; received in revised form 15 August 2007; accepted 24 August 2007

Abstract

Lipase catalysed reactions take place at the interface between the aqueous phase containing the enzyme and the oil phase. The reaction starts with the adsorption of the enzyme at the oil–water interface. In a mechanically agitated reactor, the total free interfacial area is limited and hence, there would be a critical enzyme concentration at which the interfacial area is saturated with the adsorbed enzyme. In this paper, an unsteady-state dynamic model is developed from Ping Pong Bi Bi mechanism, modified to take into consideration the effect of available interfacial area. The model is validated against experimental results from the hydrolysis of palm oil using lipase from *Candida rugusa* in a mechanically agitated batch bioreactor. It is shown that the model presented the experimental data better than previous models found in literature. The fraction of the enzyme, available in the aqueous phase, which is contributing in the coverage of oil–water interface in a stirred batch bioreactor, is determined at different agitation speeds. This fraction is found to increase as agitation speed increases, which is assumed to be a result of the increase in desorption to adsorption ratio of the enzyme at the interface with agitation.

Keywords: Lipase; Palm oil; Interfacial area; Enzymatic hydrolysis; Interfacial saturation

1. Introduction

The applications, importance and significance of lipase in oleochemical industry have been thoroughly demonstrated in literature [1–5]. The most important among these applications is the use of lipase for the production of fatty acids by hydrolysis of oils. It was recently attempted as an energy-saving method, especially for producing high value-added products or heat sensitive fatty acids [1–3].

Oil hydrolysis by lipase takes place at the interface between the aqueous phase containing the enzyme and the oil phase, where the enzyme has to be adsorbed on the oil interface as a first step in the reaction [1–3,6,7]. The lipase molecules are adsorbed and desorbed continuously at the surface of the substrate. In this dynamic system, at any instant of time, the interfacial area is partly covered with the adsorbed enzyme. On the other hand, in a mechanically stirred bioreactor, the interfacial area is affected by agitation speed, substrate concentration, and temperature [1,2,4,8]. The effects of those parameters on palm oil–water system were quantified experimentally and presented in an empirical correlation in an earlier work [8]. At any given operating condition, the total free interfacial area available is always bounded. Hence, although an increase in the bulk enzyme concentration is assumed to increase the rate of reaction, there would be a critical enzyme concentration at which the interfacial area becomes saturated with the adsorbed enzyme [8]. Beyond this point, any increase in the enzyme concentration in the bulk will enhance the reaction rate. It is essential to determine the most efficient usage of lipase, since the major obstacle to the practical exploitation of the potentials of lipase is its cost [9,10]. Unless the enzyme can be easily separated and reused, the amount of enzyme used should not exceed the critical concentration. This phenomenon of interfacial area saturation with enzyme has been demonstrated experimentally by Al-Zuhair et al. [1] for the hydrolysis of palm oil and by Albasi et al. [2] for the hydrolysis of sunflower oil. Interest of this study is focused

* Corresponding author. Tel.: +971 37133636; fax: +971 37624262.
E-mail address: S.AlZuhair@uaeu.ac.ae (S. Al-Zuhair).

1385-8947/$ – see front matter © 2007 Elsevier B.V. All rights reserved.
doi:10.1016/j.cej.2007.08.030

Nomenclature

a_t	specific total interfacial area (m^{-1})
A_m	enzyme area per unit mass ($m^2\ g^{-1}$)
C	proportionality constant
$[E]$	free enzyme concentration ($g\ m^{-3}$)
$[E_t]$	total enzyme concentration ($g\ m^{-3}$)
$[E^*]$	adsorbed enzyme concentration ($g\ m^{-3}$)
$[E^*Ac]$	adsorbed acylated enzyme complex concentration ($g\ m^{-3}$)
$[E^*P]$	adsorbed enzyme-product complex concentration ($g\ m^{-3}$)
G	glycerol moiety
k_1	reaction rate constant (min^{-1})
k_{-1}	reaction rate constant ($m^3\ mol^{-1}\ min^{-1}$)
k_2^*	reaction rate constant (min^{-1})
k_{-2}	reaction rate constant (min^{-1})
k_3	reaction rate constant (min^{-1})
k_{-3}	reaction rate constant ($m^3\ mol^{-1}\ min^{-1}$)
k_{cat}	catalytic rate constant (min^{-1})
k_d	desorption rate constant (min^{-1})
k_p	adsorption rate constant ($m\ min^{-1}$)
K_e	equilibrium constant ($mol\ m^{-3}$)
$[S]$	bulk substrate concentration ($mol\ m^{-3}$)
t	time (min)
T	temperature (K)
W_m	molecular weight of the enzyme ($g\ mol^{-1}$)

Greek letters

ϕ	volume fraction of oil in the reaction mixture
υ	reaction rate ($mol\ m^{-3}\ min^{-1}$)
ω	agitation speed (rpm)

on palm oil, due to its higher yield per hectare, compared to that of other vegetable oils, which makes it economically intuitive to consider palm oil as the feed stock for free fatty acids production [11].

2. Kinetic model

The proposed mechanism is based on the enzymatic hydrolysis mechanism presented by Bailey and Ollis [12], which shows how the reaction occurs at the active sites of the enzyme. Acidic or basic functional groups found at specific locations in the active sites of the enzyme catalyse the reaction by donating or accepting protons during the course of the reaction. The active sites of the lipase have been extensively studied by chemical and X-ray techniques [13]. Two functional groups that are part of the active sites have been identified as being particularly important to the catalytic process. One is hydroxyl group that acts as a nucleophile, and the other is the nitrogen atom of an amine group, which accepts a proton and then gives it back during the reaction. In our previous works [1,6], the enzyme was assumed to be first adsorbed on the interface, and then forms a complex with the substrate (defined the ester bond on the triglycerides) as a following step. This is applicable however, only if the substrate is dissolved in another organic solvent. In this study no organic solvent is used, and the organic phase itself represents the substrate. And as the reaction takes place at the interface, the substrate considered in this study is therefore, the specific interfacial area available per unit volume, a, which is function of agitation speed and temperature, in addition to the bulk concentration of the substrate [1,8]. Based on this, the mechanism of enzymatic hydrolysis is assumed to consist of following steps shown in Fig. 1. (a) Nucleophilic addition to form adsorbed enzyme on the substrate, the nucleophile is the oxygen in the O–H group on the enzyme. (b) Proton transfers from the conjugate acid of the amine to the alkyl oxygen atom of the substrate, and a glycerol moiety, G, is formed. If a triacylglyceride is the initial substrate, then a diacylglyceride will form, while if diacylglyceride is the substrate, then monoacylglyceride will form, and so on. (c) The oxygen atom from a water molecule is added to the carbon atom of the C=O of the acyl enzyme intermediate to form acylated adsorbed enzyme – water complex. Finally, (d) The enzyme oxygen atom of the complex is eliminated and a proton is transferred from the conjugate acid of the amine, resulting in fatty acid. These steps represent a Ping-Pong Bi Bi mechanism, and are represented in a schematic diagram shown in Fig. 2. The mechanism takes into consideration the effect of the interfacial area available by assuming the first step to be a reversible adsorption of a water-soluble enzyme at the interface producing adsorbed enzyme, E^*. The adsorption rate is assumed to be proportional to the free enzyme concentration, E, and the specific free interfacial area, a [1,3,6]. Assuming water to be in large quantities (i.e., its concentration remains constant) and according to the proposed mechanismic steps, the following rate equations are generated:

$$\frac{d[E]}{dt} = k_d[E*] + k_3[E*P] - (k_p a + k_{-3}[P])[E] \quad (1)$$

$$\frac{d[E*]}{dt} = k_p[E][a] + k_{-1}[E*Ac][G] - (k_d + k_1)[E*] \quad (2)$$

$$\frac{d[E*Ac]}{dt} = k_1[E*] + k_{-2}[E*P] - (k_{-1}[G] + k_2^*)[E*Ac] \quad (3)$$

$$\frac{d[E*P]}{dt} = k_2^*[E*Ac] + k_{-3}[E][P] - (k_{-2} + k_3)[E*P] \quad (4)$$

$$\frac{d[P]}{dt} = k_3[E*P] - k_{-3}[E][P] \quad (5)$$

$$a_t = a + A_m([E*] + [E*Ac] + [E*P]) \quad (6)$$

$$[E_t] = [E] + [E*] + [E*Ac] + [E*P] \quad (7)$$

where k_p and k_d are the enzyme adsorption and desorption rate constants, respectively, k_1 and k_{-1} are the rate constants for the reversible formation of acylated adsorbed enzyme complex,

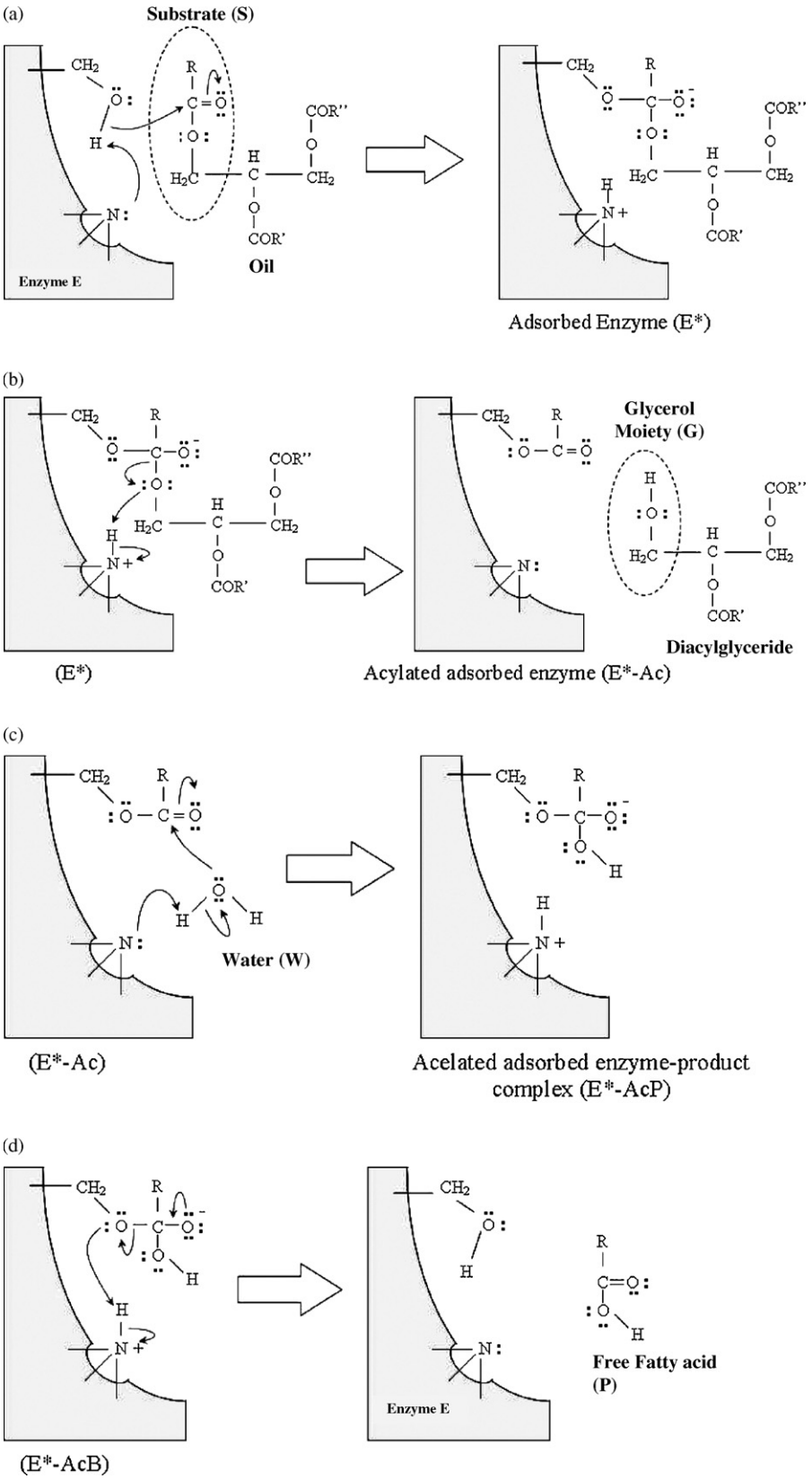

Fig. 1. The mechanism of enzymatic production of fatty acids from triacylglycerides.

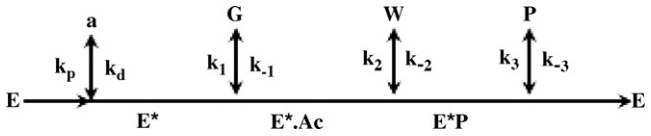

Fig. 2. Graphical representation of the mechanismic steps of triglyceride hydrolysis.

E^*Ac, k_2 and k_{-2} are the rate constants for the reversible formation of adsorbed enzyme-product complex, E^*P, k_2^* is the product of k_2 by the constant water concentration, k_3 and k_{-3} are the rate constants for the reversible formation the product and regeneration of the enzyme, a_t and a are the total and the free specific interfacial areas, respectively, $[E_t]$ is total enzyme mass concentration and A_m is the area per unit mass of enzyme. Eq. (6) is based on the assumption that all forms of the adsorbed enzyme complexes occupy the same area. This simplification is based on the fact that the enzyme has much larger volume than any molecule attached to it. It has been reported that the globular shape of lipase may be approximated by a sphere having a diameter of 50° A [7] and hence, the cross sectional area of one molecule is 2.0×10^{-17} m^2. The molecular mass of lipase is in the range of 40,000–50,000 Da and by taking an average value of 45,000 Da, the area per unit mass of enzyme is calculated to be 270 m^2 g^{-1}. It should be noted however, that lipase goes through a conformational change at the interface [7]. Therefore, the spherical shape of free enzyme is altered at the interface. In order not to over complex the analysis, this is ignored in this study.

An empirical correlation to predict the total specific interfacial area at different operating conditions was derived earlier [1,8] as shown in Eq. (8)

$$a_t(m^{-1}) = \frac{0.03\omega^{0.6}T^{1.7}[S]_o}{3303.5 + [S]_o} \pm 17\% \quad (8)$$

where ω is the agitation speed in rpm and T is the temperature in K

The series of equations (Eqs. (1)–(8)) can be solved together with the initial conditions given in Eq. (9).

$$\text{At } t = 0 : [E*] = [E*\text{Ac}] = [E*P] = [P] = 0,$$
$$\text{and } [E] = [Et] \quad (9)$$

In the proposed kinetic model, product inhibition effects are neglected, as the focus of this study was on the initial rate of reaction, where the product concentration approaches zero. In addition, substrate inhibition is also not considered, as experimental results did not show any sign of it within the substrate concentration range considered [1].

Al-Zuhair et al. [6] proposed simplified mechanismic steps with pseudo-steady state assumption (i.e., constant intermediate concentrations) to derive the following expression:

$$\upsilon = \frac{((k_{cat}^* a_t)/A_m)[S]}{K_e + [S]}(G_1 - G_2) \quad (10)$$

where υ is the initial rate of reaction, and k_{cat} is rate constants for the irreversible formation the product, C is proportionality constant,

$$K_e = \frac{(k_{cat} + k_{-1})}{k_1} \quad (11)$$

$$k_{cat}^* = \frac{k_{cat}}{2CW_m} \quad (12)$$

$$G_1 = \frac{(k_d/k_p)}{a_t^2[1 + ([S]/K_e)]} + 1 + \left(\frac{A_m}{a_t}\right)[E_t] \quad (13)$$

and

$$G_2 = \left(G_1^2 - \frac{4(A_m)_m(E_t)_m}{a_t}\right)^{0.5} \quad (14)$$

The Eqs. ((10)–(14)) were used to predict the hydrolysis rate of oils by lipase at any enzyme concentration. On the other hand, Al-Zuhair et al. [1] derived a simpler form of Eq. (10) applicable for low enzyme concentrations, where the coverage of the total area with enzyme molecules was assumed negligible,

$$\upsilon = \frac{k_{cat}^*[E_t][S]}{K_e[(k_d)/(k_p a_t^2) + 1] + [S]} \quad (15)$$

3. Materials and methods

3.1. Materials

The experimental results from our previous work [1] for the hydrolysis of palm oil in well-agitated bioreactor are used. Refined palm oil used in this study was obtained from Lam Soon (M) Buruh, Malaysia. The substrate considered is the ester bond on the triglyceride. Lipase from *Candida rugosa* was obtained from Sigma Chemical Co., Japan. The reuse of lipase is essential from the economic point of view, which can be achieved by using the lipase in immobilised form. However, soluble enzyme and not immobilised is purposely used in this study to avoid the mass transfer limitations or clogging problems, which could complicate the kinetic model. Using soluble lipase has the advantage of having the interaction with the substrate be at molecular level, with no mass transfer limitations or clogging problems. Therefore, it is justified to assume negligible external mass transfer resistance in the subsequent analysis. The model derived in this study can be used to determine a mass transfer resistance of immobilised enzyme of the same strain, however, this is beyond the scope of this paper.

3.2. Experimental set-up

The reactor used is a 0.6 l batch stirred bioreactor with a working volume of 400 ml. A four-bladed paddle impeller immersed in the solution at one-third-depth level was used for agitation. The initial rate of palm oil hydrolysis was determined by titrating the extracted fatty acids against 0.05 N NaOH solution in isopropanol, using an auto-titrator (Metrohm 702 SM titrino). The results were verified by comparing them to those found by gas chromatograph (Chemito GC 8610). The comparison showed that the average difference between the readings of the

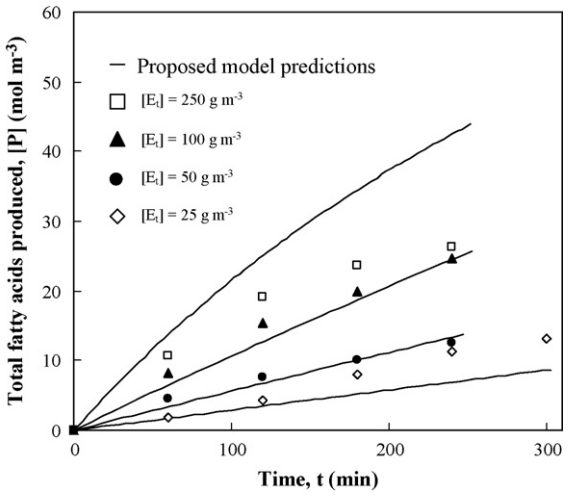

Fig. 3. Fatty acid production at $\omega = 800$ rpm.

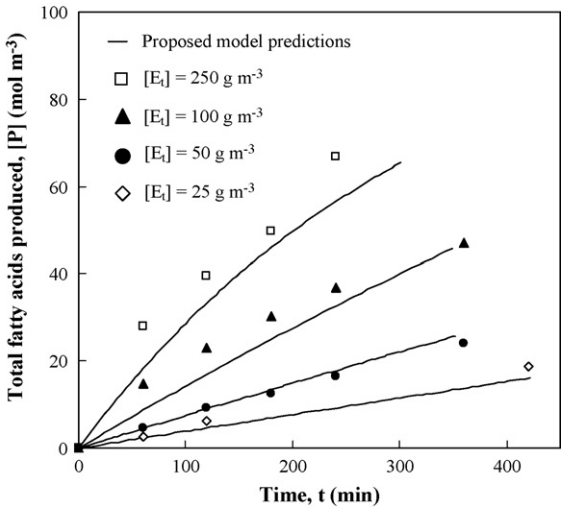

Fig. 5. Fatty acid production at $\omega = 1300$ rpm.

two methods was less that 10%. The effects of different parameters on the initial hydrolysis rate were determined [1]. These parameters included: initial substrate concentration, temperature, agitation speed and initial enzyme concentration. Other experimental and analysis details are found elsewhere [1].

In this work, the results at constant initial substrate concentration of 660.7 mol m^{-3} and the optimum temperature of 318 K [1] are only considered, as the effects of their changes are not of significant importance to this work. On the other hand, the effect of enzyme concentration in the range of 25–250 g m^{-3} and stirrer speed in the range of 800–1300 rpm, are considered.

4. Results and discussion

The time courses for the production of fatty acids produced are shown in Figs. 3–5. The initial rate of reaction at each agitation speed and enzyme concentration is determined from the slope of the best fit of the initial linear region of the product concentration curve using Excel. Fig. 6 shows the effect of increasing enzyme concentration, on the initial rate of reaction at different agitation speeds. The solid lines in Fig. 6 are connections between the experimental data, shown to highlight the trend. It can be seen that the initial rate of reaction increases linearly with the enzyme concentration at low enzyme concentrations, while this increase tends to decrease at high enzyme concentrations. This phenomenon is most probably caused by the considerable reduction in the available interfacial area, as most of it would be covered with different enzyme complexes molecules and further increase in bulk concentration of the enzyme does not result in a corresponding increase in the initial reaction rare. Similar trend is also observed in the result of Albasi et al. [2] for the hydrolysis of sunflower oil with lipase. Fig. 6 also shows that the critical enzyme concentration, at which the effect of enzyme concentration on the initial rate fades, increases as the agitation speed increases. For example, at an agitation speed of 800 rpm, the area was saturated at enzyme concentration of about 95 g m^{-3}, whereas interfacial saturation played a dominant role at enzyme concentrations above 100 g m^{-3} and above 250 g m^{-3} for agitation speeds, ω, of 1000 and 1300 rpm, respectively. The reason for this was assumed in our earlier work [1]

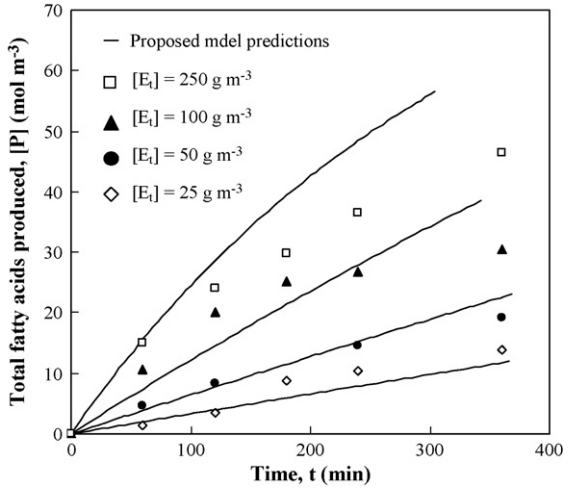

Fig. 4. Fatty acid production at $\omega = 1000$ rpm.

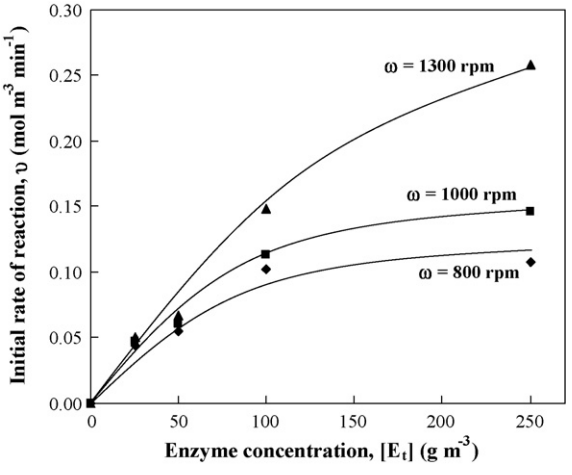

Fig. 6. Effect of enzyme concentration on the initial rate of reaction at different stirrer speeds (reproduced from [1]).

Table 1
Reaction rate constants and an expression of the total specific interfacial area reported by Al-Zuhair et al. [1]

Parameter	Value
k^*_{cat} (min^{-1})	1.8×10^{-3}
K_e (mol m^{-3})	5.65
k_d/k_p (m^{-2})	7.7×10^7

to be due only to the increase in the interfacial area available at higher agitation speeds. However, in this work, it is shown that this is not the sole reason, as discussed in Section 7.

The previous model equations (Eqs. (10)–(15)) were solved together with the interfacial area correlation (Eq. (8)), using the rate constants presented in Table 1. The values of the rate constants were obtained from the experimental results by multiple regression method using MATLAB [1]. Fig. 7 shows a comparison between high enzyme and low enzyme model predictions at 1300 rpm [6]. It can be seen that the high enzyme concentration model follows the trend of the experimental data and shows the effect of interfacial area saturation. However, the results are considerably underestimated and the relative standard deviation between the high enzyme model prediction and the experimental results is ±0.345. On the other hand, the low enzyme model curve deviates from the experimental data at high enzyme concentrations and do not predict the interfacial area saturation. Similar results are observed for model predictions at other agitation speeds, which are found elsewhere [6]. Therefore, it is obvious that both previous models, namely, high and low enzyme models, do not predict the data well and the development of a more reliable kinetic model is still needed.

5. Determination of kinetic parameters

The set of equations (Eqs. (1)–(7)) proposed in this study are solved numerically together with Eq. (8) by the Runge–Kutta–Fehlberg algorithm using POLYMATH computer software. The numerical technique was subjected to a constraint that k_d/k_p ratio should equal 7×10^7 to comply with the kinetic parameters found in Table 1. The accuracy requested was that both the relative and absolute (maximal) errors be less than the truncation error tolerance, which was set to be 1.0×10^{-6}. The initial conditions used were those shown in Eq. (9). The equations are solved for different operating conditions to determine the kinetic parameters that result in the best presentation of the experimental data. The kinetic parameters were optimised using Excel spreadsheet to find the minimum objective function (Eq. (16)) that compares the measured product concentration with that predicted by the proposed kinetic model.

$$\mathrm{OF} = \sum ([P]_{\mathrm{pred}} - [P]_{\mathrm{expt}})^2 \tag{16}$$

The values of the kinetic parameters determined in this study are shown in Table 2. Figs. 3–5 show comparison between the experimental results and the kinetic model prediction for agitation speeds of 800, 1000 and 1300 rpm, respectively. In general, the figures show that the kinetic model predictions of the experimental data are moderately acceptable. A considerable deviation between the experimental data and the model predictions is observed at very high enzyme concentration of 250 g m^{-3}, however, this deviation reduces as agitation speed increases to reach a minimum at agitation speed of 1300 rpm (Fig. 5). On the other hand, it is not possible to compare between the values of the kinetic parameters found in this study with those found in previous studies as their definitions and dimensions are different.

The values of the product concentration predicted by the proposed model equations (Eqs. (1)–(7)) are used to determine the initial rate of reaction using Excel. The initial rate of reaction at each initial substrate concentration is determined from the slope at time zero of the straight line that best fit product concentration versus time data. Figs. 7 and 8 show a comparison between the values of the initial rate of reaction determined experimentally with those determined from the proposed model at two agitation speed of 1300 and 800 rpm, respectively. The results show that the proposed model predicted very well the initial rate of reaction at agitation speed of 1300 rpm, however, the predictions slightly overestimates the experimental values at agitation speed of 800 rpm, especially at high enzyme concentrations. Comparison between the current model predictions with those of the high enzyme and low enzyme models shows that the current model predictions of the initial rate of reaction are much better. At agitation speed of 1300, the average standard deviation of the current model is ±0.049, which is more than

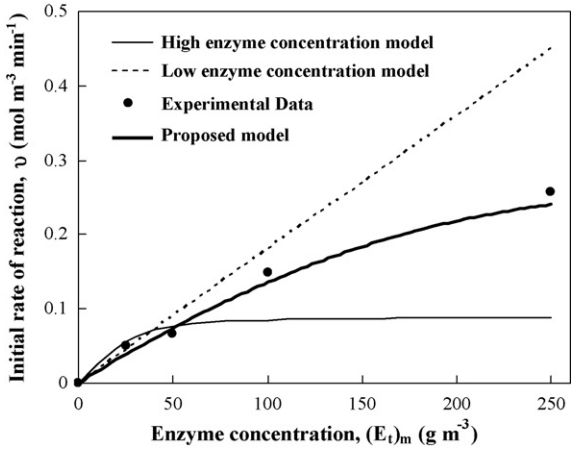

Fig. 7. Comparison between predictions of the initial rate of reaction using high enzyme and low enzyme models and the proposed model at $\omega = 1300$ rpm.

Table 2
Values of the rate constants

Rate constant	Value
k_p (m min^{-1})	9.0×10^{-7}
k_d (k_p min^{-1})	7.7×10^7
k_1 (min^{-1})	21.5
k_{-1} (m^3 mol^{-1} min^{-1})	0.01
k^*_2 (min^{-1})	13
k_{-2} (min^{-1})	0.01
k_3 (min^{-1})	73
k_{-3} (m^3 mol^{-1} min^{-1})	0.05

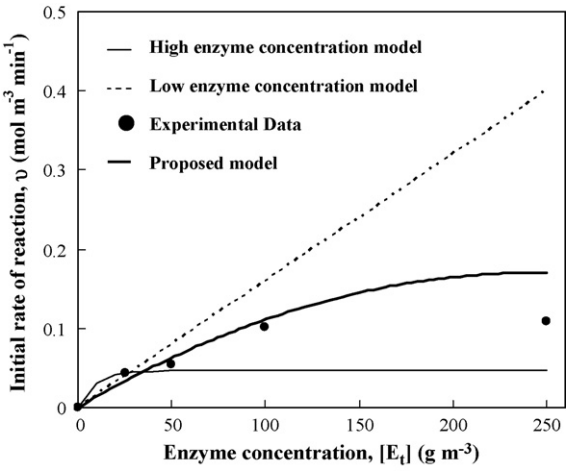

Fig. 8. Comparison between predictions of the initial rate of reaction using high enzyme and low enzyme models and the proposed model at $\omega = 800$ rpm.

seven times lower than that of the high enzyme concentration model, ±0.345. At 800 rpm, the accuracy of predictions of the proposed model reduces to give an average standard deviation of ±0.21. However, this value is still better than that of the high enzyme concentration model, ±0.27. Therefore, the new model equations (Eqs. (1)–(9) are more appropriate for predicting the initial rate of hydrolysis of palm oil at any substrate and enzyme concentrations and can be used to design batch or continuous bioreactors and to determine the optimum operating conditions.

6. Changes in intermediates concentration

The change of the concentrations of each intermediate is calculated by solving the set of equations (Eqs. (1)–(7)), and the results are shown in Fig. 9 for $\omega = 800$ rpm and $[E_t] = 250\ g\ m^{-3}$. Similar results are observed for other agitation speeds and enzyme concentrations. However, the lowest agitation speed and highest enzyme concentration are chosen to be shown in Fig. 9, because they demonstrate the most perceptible changes. The figure shows the changes in the intermediate concentrations are not large; nevertheless, they do not reach their steady state throughout the time considered. Fig. 9a shows that the concentration of the adsorbed enzyme [E^*] reaches a maximum at around 14 min then drop gradually after that. The initial increase is because of the combined effects of high free enzyme concentration, large free interfacial area available for adsorption and low [E^*] decomposition reactions (i.e., desorption and formation the intermediate [E^*Ac]) due to its initial low amounts. However, after some time (15 min), enough [E^*] is formed and its decomposition reactions become higher than its formation reaction, which is mainly due to the reduction in interfacial area available. Fig. 10 shows the changes in the free specific interfacial area with time at $\omega = 800$ rpm and $[E_t]$ of 25 and 250 g m^{-3}. The results in Fig. 10 show a sharp drop in the specific free interfacial area at $[E_t]$ of 250 g m^{-3}, whereas this effect is negligible at lower enzyme concentration of 25 g m^{-3}. This results support the interfacial area saturation hypothesis assumed in our previous works [1,6]. On the other hand, Figs. 11 and 12 show the

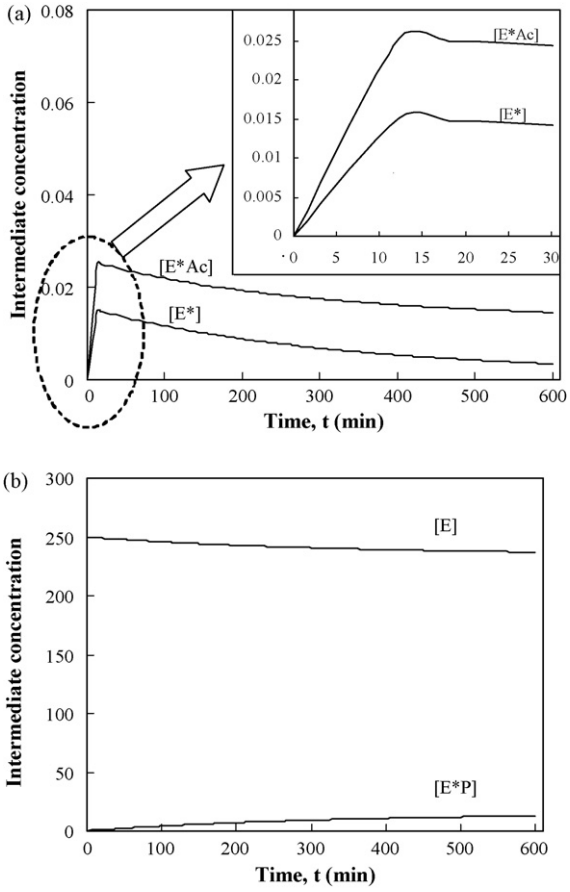

Fig. 9. The change in intermediate concentrations with time at $\omega = 800$ rpm and $[E_t] = 250\ g\ m^{-3}$.

effects of changing $[E_t]$ and ω on the adsorbed enzyme concentration, [E^*], respectively. It is found that increasing $[E_t]$ and/or ω results in increasing the maximum value of [E^*] but does not affect time it takes to reach this maximum. In addition it is found that $[E_t]$ and ω have no effect on the equilibrium concentration of the adsorbed enzyme. Fig. 11 shows that at low initial enzyme concentration of 25 g m^{-3}, the drop in the concentration of [E^*] was much less that that at high initial enzyme concentration

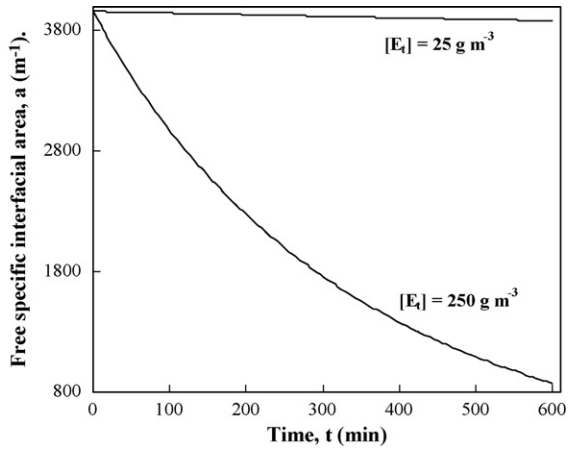

Fig. 10. The specific free interfacial area, a, at $\omega = 800$ rpm and $[E_t] = 25$ and 250 g m^{-3}.

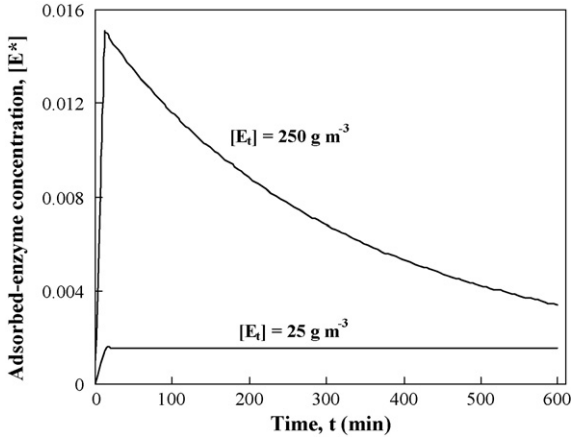

Fig. 11. The concentration of adsorbed enzyme [E^*] at $\omega = 800$ rpm and [E_t] = 25 and 250 g m^{-3}.

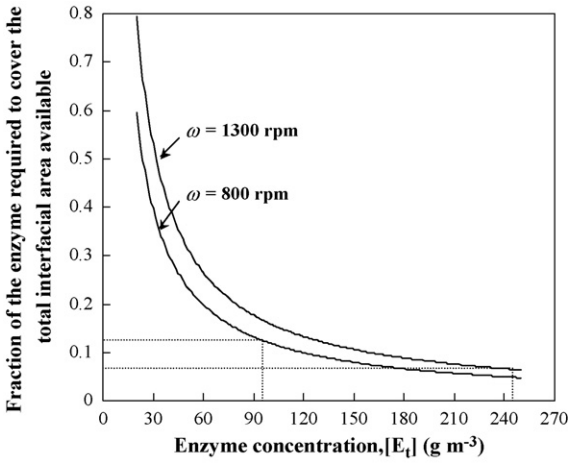

Fig. 13. The Effect of stirrer speed on the fraction of enzyme required to fully cover the available interfacial area.

of 250 g m^{-3}. This is mainly because of the large free specific interfacial area available for enzyme to be adsorbed as shown in Fig. 10. The results in Figs. 10 and 11 suggest that that the pseudo-steady state assumption used in the development of the high enzyme concentration model [6] is acceptable only at low [E_t], however, the assumption is clearly oversimplified at higher values of [E_t]. This explains why the high enzyme model [6] followed the experimental results better at low values of [E_t], and showed a consistent offset at high values of [E_t].

7. Fraction of the enzyme at the interface

The fraction of enzyme in solution needed to fully cover the interfacial area is determined using the experimental results shown in Fig. 6, Eq. (8) and the value of A_m. The results are shown in Fig. 13 for two agitation speeds, namely 800 and 1300 rpm. The trend is similar at agitation speeds of 1000 rpm, but it is not included to avoid congestion. The y-axis shows the fraction of the total enzyme whose area, at a specific enzyme concentration, is equal to the total interfacial area generated at a specific agitation speed. The dashed lines indicate the points

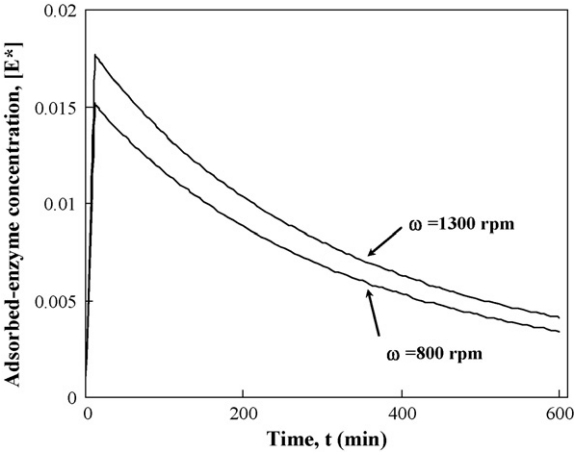

Fig. 12. The concentration of adsorbed enzyme [E^*] at [E_t] = 250 g m^{-3} and $\omega = 800$ and 1300 rpm.

where the enzyme saturates the available interfacial area as found from Fig. 6. It can be seen that the enzyme at the interface represents 12% of the total enzyme available in the bulk at the agitation speed of 800 rpm and decreases to 6% at the agitation speed of 1300 rpm. It should be noted however, that lipase goes through a conformational change at the interface [7]. Therefore, the spherical shape of free enzyme is altered at the interface, and the fractions of lipase actually needed to totally saturate the interface at each agitation speed, are less that those predictions shown above. Nevertheless, the predictions still give good basis for comparison. The results show that at lower agitation speeds, a larger portion of the enzyme in the aqueous solution is utilised in the reaction. Hence, although increasing the agitation speed results in higher reaction rate, in view of efficient usage of the enzyme, lower agitation speeds tends to be favourable. This proves that the high enzyme concentration required to fully saturate the available interfacial area at high agitation speeds is not solely due to the increase in the interfacial area as was assumed earlier [6]. However, it is also due to the ineffective utilisation of the enzyme at higher agitation, where smaller portion of the enzyme are actually contributing to the reaction. This explanation is further strengthened by comparing the percentage increase in interfacial area of 15% (from 3963 to 4531 m^{-1}) when mixing speed increases from 800 to1000 rpm, and by almost the same percentage, 17% (to 5303 m^{-1}) when the mixing speed increases to 1300 rpm. However, Fig. 6 shows that the apparent saturation concentration of enzyme increases slightly from 95 to 100 g m^{-3} as agitation speed increases from 800 to 1000 rpm, but significantly to above 250 g m^{-3} as agitation speed reaches 1300 rpm. In other words, the concentration at which the interface becomes saturated is not proportional to the interfacial area as assumed earlier [6]. The other factor that plays role in this is the ratio of the adsorption to the desorption constants. This ratio decreases at higher agitation speeds, due to physical erosion and faster deformation of the droplets, which results in lower adsorbed enzyme molecules on the interface. Nevertheless, in Section 5, the ratio of k_d/k_p was taken constant at different agitation speeds to simplify the calculations.

8. Conclusion

Mathematical model is developed to predict the reaction dynamics of enzymatic palm oil hydrolysis. The model takes into consideration the influence of enzyme molecule coverage of the interfacial area. The effects of initial enzyme concentration and agitation speed are measured experimentally and compared to the proposed model predictions. The proposed model presented the experimental data better than previous models found in literature. In addition, under different operation conditions, the fraction of the enzyme, available in the aqueous solution, which is contributing to the interfacial coverage, has been determined experimentally. It is found that the amount of enzyme needed to cover the interface increases as the agitation speed increases, due to combination effects of increased area available and ineffective utilisation of enzyme at higher agitation speeds.

References

[1] S. Al-Zuhair, M. Hasan, K.B. Ramachandran, Kinetics of the enzymatic hydrolysis of palm oil by lipase, Proc. Biochem. 38 (2003) 1155–1163.
[2] C. Albasi, N. Bertrand, J.P. Riba, Enzymatic hydrolysis of sunflower oil in a standardized agitated tank reactor, Bioprocess. Eng. 20 (1999) 77–81.
[3] S.W. Tsai, C.S. Chang, Kinetics of lipase-catalysed hydrolysis of lipids in biphasic organic–aqueous systems, J. Chem. Tech. Biotechnol. 57 (1993) 147–154.
[4] A.W. Pacek, C.C. Man, A.W. Nienow, On the Sauter mean diameter and size distribution in turbulent liquid/liquid dispersions in a stirred vessel, Chem. Eng. Sci. 53 (1998) 2005–2011.
[5] G. Zhou, S.M. Kresta, Correlation of the mean drop size and minimum drop size with the turbulence energy dissipation and the flow in an agitated tank, Chem. Eng. Sci. 53 (1998) 2063–2079.
[6] S. Al-Zuhair, M. Hasan, K.B. Ramachandran, High enzyme concentration model for the kinetics of hydrolysis of oils by lipase, J. Chem. Eng. 103 (2004) 7–11.
[7] R. Verger, C.E. Maria, G.H. DeHaas, Action of phospholipase A at interfaces, J. Biol. Chem. 218 (1973) 4028–4034.
[8] S. Al-Zuhair, K.B. Ramachandran, M. Hasan, Investigation of the specific interfacial area of palm oil/water system, J. Chem. Technol. Biotechnol. 79 (2004) 706–710.
[9] M.V. Arbidge, W.H. Pitcher, Industrial enzymology: a look towards the future, Trends Biotechnol. 7 (1989) 330–335.
[10] S. Mukataka, K. Tetsuo, T. Joji, Kinetics of enzymatic hydrolysis of lipids in biphasic organic-aqueous systems, J. Ferment. Technol. 63 (1985) 461–466.
[11] J. Tickell, From the Fryer to the Fuel Tank: The Complete Guide to Using Vegetable Oil as an Alternative Fuel, third ed., FL Tickell Energy Consulting, 2000.
[12] J.E. Bailey, D.F. Ollis, Biochemical Engineering Fundamentals, 2nd edition, McGraw Hill, 1986.
[13] I. Panalotov, R. Verger, Physical Chemistry of Biological Interfaces, Marcel Dekker Inc., New York, 2000.